The Wiener–Khinchin theorem and recurrence quantification

Joseph P. Zbilut [a],[*], Norbert Marwan [b]

[a] *Department of Molecular Biophysics and Physiology, Rush University Medical Center, 1653 W. Congress, Chicago, IL 60612, USA*
[b] *Potsdam Institute for Climate Impact Research (PIK), 14412 Potsdam, Germany*

A R T I C L E   I N F O

A B S T R A C T

The Wiener–Khinchin theorem states that the power spectrum is the Fourier transform of the autocovariance function. One form of the autocovariance function can be obtained through recurrence quantification. We show that the advantage of defining the autocorrelation function with recurrences can demonstrate higher dimensional dynamics.

© 2008 Published by Elsevier B.V.

1. Introduction

Recurrence plots (RP) and techniques related to RPs have become popular in the last two decades for its unique abilities to discern subtle processes, especially in the case where the requirements for classical techniques such as the Fourier transform (FT) are not met; i.e., stationarity, linearity, and/or where the dynamics reside in higher dimensional spaces [1–3,5]. In a previous letter we demonstrated that a recurrence spectrum can show sharp frequency components not easily resolved with the FT [4]. A drawback was the "noise" clutter due to the high resolution. The present Letter shows that this problem can be obviated by using the two techniques together due to the well-known Wiener–Khinchin theorem. The theorem states that the power spectral density of a wide-sense-stationary random process is the Fourier transform of the corresponding autocovariance function [6].

2. Power spectral estimate by recurrences

The power spectrum of a deterministic, finite length, discrete-time signal, $x(i)$, is the magnitude squared of the signal's Fourier transform

$$S_x(\omega) = \frac{1}{N} \left| \sum_{i=0}^{N-1} x(i) e^{-j\omega i} \right|^2. \tag{1}$$

Using the Wiener–Khinchin theorem, the power spectrum of a signal equals the Fourier transform of the autocovariance function C_x of the signal:

$$S_x(\omega) = \sum_{\tau=-\infty}^{\infty} C_x(\tau) e^{-j\omega\tau}, \tag{2}$$

where the autocovariance function of a stochastic time series $x(n)$ is defined as

$$C_x(\tau) = \frac{1}{N} \sum_{i=0}^{N-1-\tau} x(i) x^*(i+\tau). \tag{3}$$

The calculation of a RP from phase space vectors $\vec{x}(i) \in \mathcal{R}^m$ ($i = 1, \dots, N$ and m the dimension of the system) is based on the distance matrix **D** of the pair-wise distances between all data points (state space vectors):

$$D(i, j) = \left\| \vec{x}(i) - \vec{x}(j) \right\| \quad \text{with } \vec{x} \in \mathcal{R}^m. \tag{4}$$

For single dimensional observations x, we may consider embeddings of the time series with embedding dimension m [7]. [For the following equations until Eq. (8), $m = 1$.]

* Corresponding author. Tel.: +1 312 942 6008; fax: +1 312 942 8711.
E-mail address: jzbilut@rush.edu (J.P. Zbilut).

The average of the distance values $d(\tau)$ for a given lag τ defined as

$$d(\tau) = \frac{1}{N} \sum_i D(i, i + \tau),\qquad(5)$$

can be considered as a generalization of the autocovariance. In fact, the distance matrix can be directly related to the autocovariance $C_x(\tau)$ [8]. For this purpose we consider the squared distance matrix

$$
\begin{aligned}
D^2(i, i + \tau) &= \|x(i) - x(i + \tau)\|^2 \\
&= \big(x(i) - x(i + \tau)\big)\big(x(i) - x(i + \tau)\big) \\
&= x^2(i) - 2x(i)x(i + \tau) + x^2(i + \tau).
\end{aligned}\qquad(6)
$$

Next we calculate $d(\tau)$ from $\mathbf{D}^2$ and get

$$
\begin{aligned}
&\frac{1}{N} \sum_i D^2(i, i + \tau) \\
&= \frac{1}{N}\left(\sum_i x^2(i) - \sum_i 2x(i)x(i + \tau) + \sum_i x^2(i + \tau) \right) \\
&= \sigma^2 - C_x(\tau) + \sigma^2 \\
&= 2\big(\sigma^2 - C_x(\tau)\big)
\end{aligned}\qquad(7)
$$

and find as the relation between $C_x(\tau)$ and D^2

$$\frac{1}{2}d^2(\tau) - \sigma^2 = -C_x(\tau),\qquad(8)$$

with σ^2 as the variance of the data. Obviously, the average distance $d(\tau)$ corresponds to the auto covariance up to a shift by the variance and the factor $1/2$. Note that we have considered the squared distance matrix. However, the sign flip also remains for the simple distance matrix, because the distance matrix consists only of positive values, and, therefore, the quadrature of $\mathbf{D}$ has no effect on the sign.

Considering embedding dimensions $m > 1$, embedding delay 1, and using the Euclidean norm, the squared distance matrix $\mathbf{D}^2$ is calculated by

$$
\begin{aligned}
D^2(i, i + \tau) &= \|\vec{x}(i) - \vec{x}(i + \tau)\|^2 \\
&= \sum_{k=1}^m \big(x_k(i) - x_k(i + \tau)\big)\big(x_k(i) - x_k(i + \tau)\big) \\
&= \sum_{k=1}^m \big(x_k^2(i) - 2x_k(i)x_k(i + \tau) + x_k^2(i + \tau)\big) \\
&= \|\vec{x}(i)\|^2 - 2\vec{x}^*(i)\vec{x}(i + \tau) + \|\vec{x}(i + \tau)\|^2.
\end{aligned}\qquad(9)
$$

The term $\vec{x}^*(i)\vec{x}(i + \tau)$ corresponds to the autocovariance of the segment of the time series for time $i, i + 1, \ldots, i + (m - 1)$. Moreover, by summarizing over index i (and for large N), we find that

$$\sum_i \vec{x}^*(i)\vec{x}(i + \tau) = m \sum_i x(i)x(i + \tau);\qquad(10)$$

i.e., it corresponds to the autocovariance up to a factor of mN.

However, here we propose to go one step further and to consider only recurrences, defined by applying a threshold to the distance matrix $\mathbf{D}$. This limits the matrix to periodic orbits:

$$\mathbf{R} = \Theta(\varepsilon - \mathbf{D});\qquad(11)$$

i.e., $\mathbf{R}$ is then the recurrence matrix. Then we consider the probability that the system recurs after time τ (τ recurrence rate) [5,9]

$$RR(\tau) = \frac{1}{N - \tau} \sum_{i=1}^{N-\tau} R(i, i + \tau),\qquad(12)$$
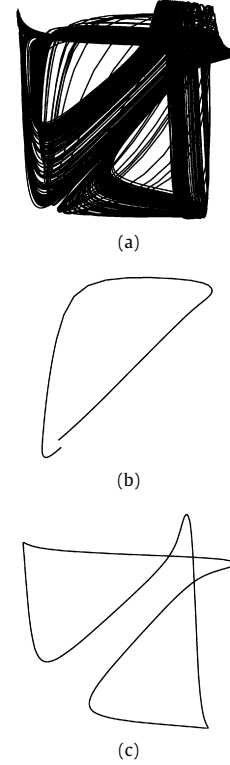
Fig. 1. (a) The BZ reactor (50 000 points). (b) Trajectory near saddle-1. (c) Trajectory near saddle-2.

and replace $C_x(\tau)$ in Eq. (2) by $RR(\tau)$. In other words, we replace the expectation values

$$E\big\{x(i)x^*(i + \tau)\big\} \longrightarrow E\big\{\Theta\big(\varepsilon - \|\vec{x}(i) - \vec{x}(i + \tau)\|\big)\big\}.\qquad(13)$$

The putative advantages of using a recurrence-derived FT includes not only its relaxed assumptions of stationarity and nonlinearity, but also its use of the embedding theorem to capture dynamics of higher dimensional spaces. Thus, periodicities are demonstrated not seen in either the regular FT periodogram, or the (standard) autocovariance-derived Fourier transform. Additionally, there is the "smoothing" effect inherent in the FT. (Whereas we use the autocovariance, it should be noted that the autocorrelation can also be used, since it is simply the normalization of the autocovariance by the total autocovariance.)

3. Example

We illustrate the advantage of the proposed recurrence based Fourier spectrum with an example of high dimensional dynamics. Lathrop and Kostelich previously studied the attractor of the oscillating Belousov–Zhabotinsky (BZ) chemical reaction [10,11], which is possibly chaotic. The bromide ion concentration was recorded, and a phase-space strange attractor was constructed from the method of time-delays. Their analysis recommended an embedding of 3, and a delay of 124. Further analysis of 3-dimensional recurrences demonstrated saddle orbits of period-1, -2 and -3 (Fig. 1). The fundamental period was approximately 125 time steps.

To determine if the recurrence plot (RP)-based FT could capture these periods, a sample of 1 000 points was selected from the original data, and submitted to the technique. We used the suggested embedding (dimension 3, and delay 124), and a recurrence threshold ε of 0.75. We also calculated a standard FT spectrum (rectangular window, no overlapping) and the autocovariance-based FT.
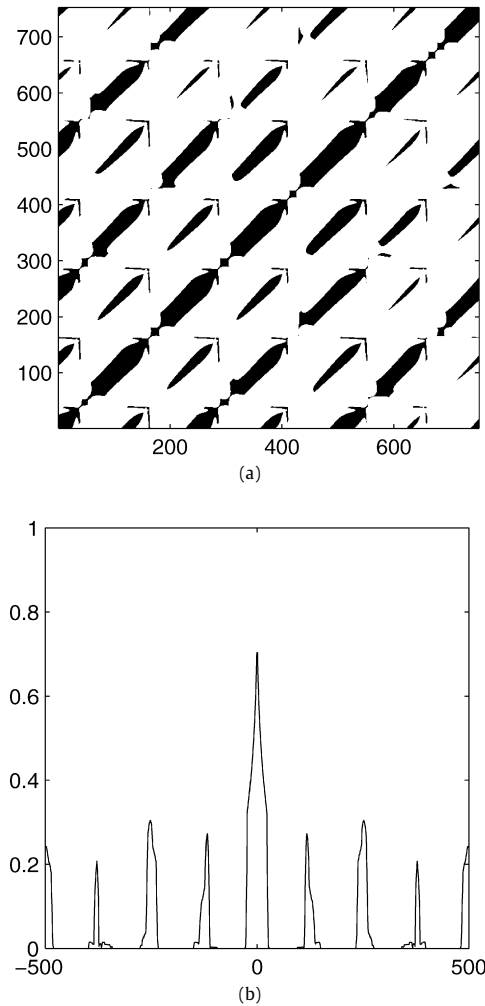
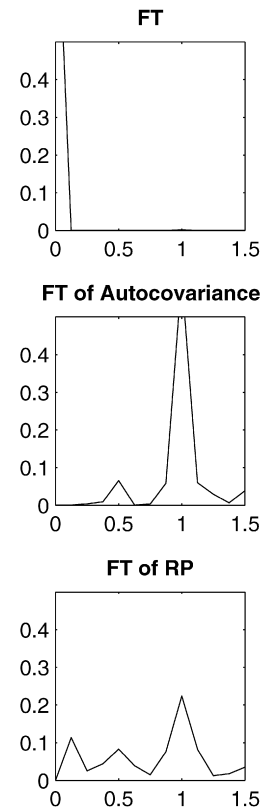Fig. 2. (a) Recurrence plot for 1 000 points of the BZ reactor. (b) Recurrence spectrum derived from the Plot.

Fig. 3. Power spectra of 1 000 points of BZ reactor with frequency normalized to saddle-1 and power normalized to total power. (Top) FT spectrum with rectangular window. (Middle) Autocovariance based spectrum. (Bottom) RP-based spectrum.

The RP of the BZ data reveals periodically occurring structures of different width and length (Fig. 2(a)), depending on the different periodic orbits. These periodically occurring structures are measured by the recurrence spectrum [Eq. (12)] (Fig. 2(b)). Note that although the peaks are relatively sharp, they are not smooth due to the thresholding, ε.

Next we apply the FT on the recurrence spectrum (Fig. 3(c)). The RP-based FT not only demonstrates the fundamental, but also the period-2 (near 0.5), as well as a period-3 (near 0.2–0.25). These peaks have been smoothed by the application of the FT.

By contrast, the standard FT does not demonstrate any significant peaks (broad band noise is seen with log scales–not shown). The autocovariance-based FT does show the fundamental frequency, plus a period-2 (near 0.5), but is not able to find the period-3. Only the RP-based FT is able to detect all the period-1, -2 and -3 orbits in the dynamics of the BZ system.

4. Discussion and conclusion

We have proposed an alternative technique for the detection of periodicities in dynamical systems based on recurrences. Applying the FT on the probability that a state recurs after certain time, also known as the τ-recurrence rate [5], we link recurrence quantification with spectral analysis. In the present study we used 1 000 points to limit computational time. When other 1 000 point segments were chosen, the frequencies shifted due to the sampling of

different sections of the attractor (see Fig. 1, also Fig. 4). Thus it is important to estimate the extent of the attractor, in order to avoid making the conclusion that the dynamics are nonstationary as a result of inadequate sampling. (See also [12].)

Another consideration is the choice of embedding dimension. In the present example the choice was made for $m = 3$ in keeping with the analysis of Lathrop and Kostelch. A comprehensive discussion of the subject is beyond the scope of this Letter, and the interested reader is referred to [5] for a fuller discussion. However, we did perform a brief analysis with results in Fig. 5. For embeddings 1 to 2 the FT and autocovariance-based FT remain the same, while the RP-based FT reveals new peaks until reaching the putatively correct embedding of 3. At an embedding of 4, however, the plot begins to diminish and the peaks are smoothed out. This occurred even with adjusting the value of ϵ in accordance with the recognition of the "curse of dimensionality". (Results not shown.) This suggests a practical method of determining an appropriate embedding once a delay via mutual information has been established: increasing the embedding beyond the optimal embedding simply brings in more points whose dynamics begin to obscure the true close in points, since the points tend to be distributed over a more narrow range of the interior of an m-dimensional hypersphere. And as $m \to \infty$, the standard deviation of the inter-point distances approaches 0 [13]. Thus one can increase the embedding until such a result is encountered. Certainly, additional research is required to confirm this observation.

One drawback of the technique is that the RP-based FT may require extended computational time with either long or highly embedded dynamics. Nonetheless, when oscillatory dynamics are suspected which move in higher dimensions, it might be useful to consider the RP-based FT.
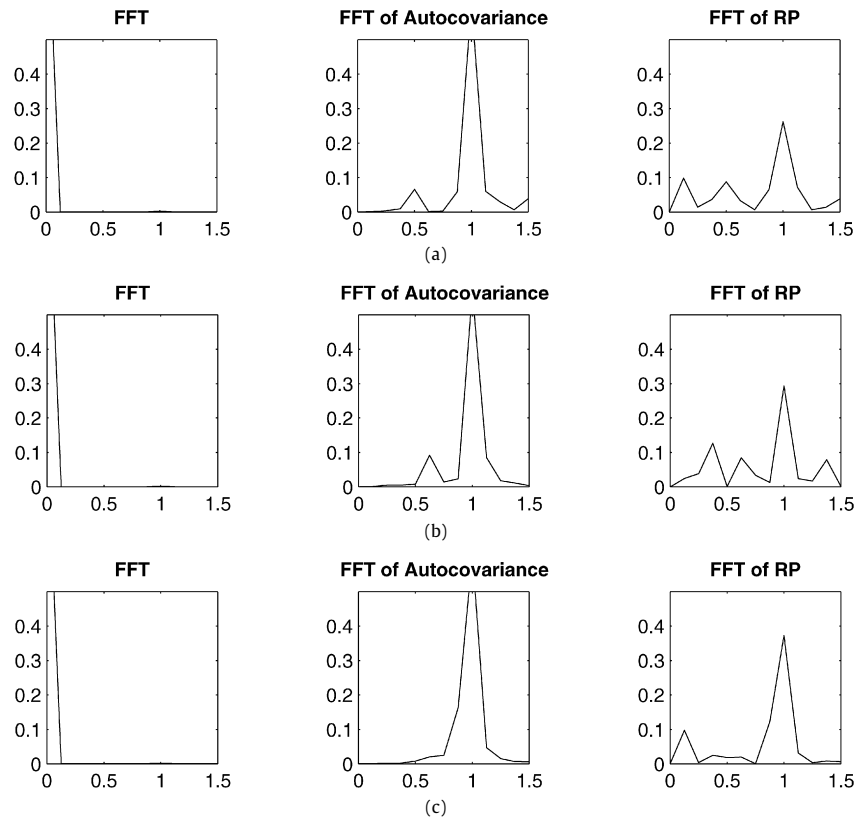
Fig. 4. Result of analyzing three sequential series of 1 000 points (a)–(c) of the BZ attractor. This is due to inadequate sampling of the total extent of the attractor as seen in Fig. 1.
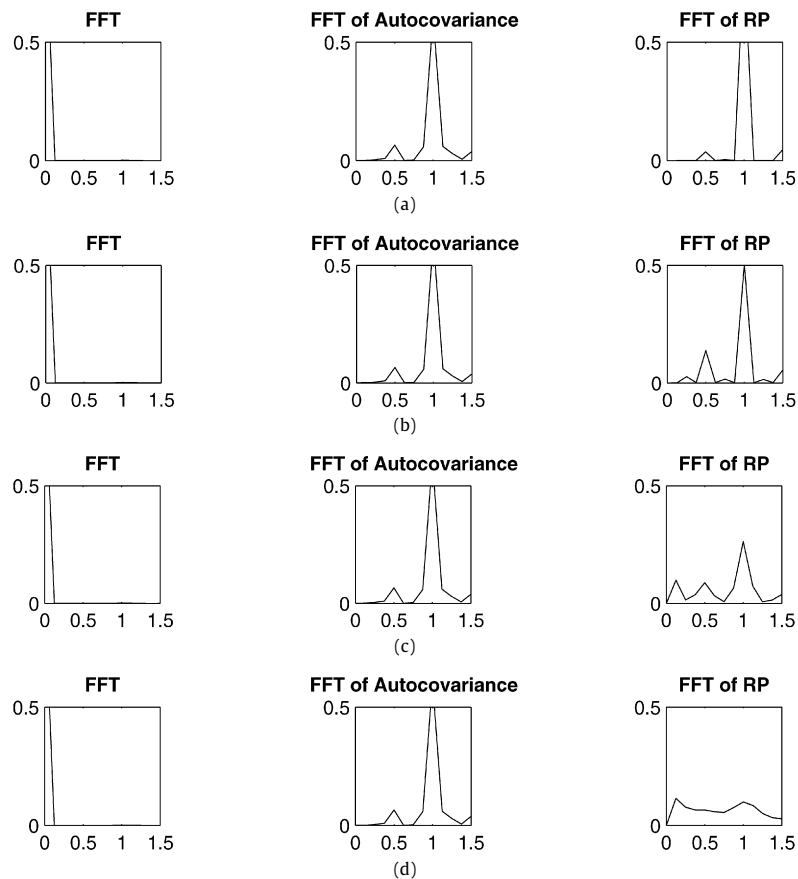
Fig. 5. Results for progressive embedding of the time series from 1 to 4 (a)–(d). The correct periods are found for an embedding of 3, but are obscured with an embedding of 4.

References

[1] J.P. Zbilut, C.L. Webber Jr., Int. J. Bifur. Chaos 17 (10) (2007) 3477.

[2] J.P. Zbilut, C.L. Webber Jr., Recurrence quantification analysis, in: M. Akay (Ed.), Wiley Encyclopedia of Biomedical Engineering, John Wiley & Sons, 2006.

[3] C.L. Webber Jr., J.P. Zbilut, Recurrence quantification analysis of nonlinear dynamical systems, in: M.A. Riley, G.C. Van Orden (Eds.), Tutorials in Contemporary Nonlinear Methods for the Behavioral Sciences Web Book, National Science Foundation, US, 2005, pp. 26–94.

[4] K. Shockley, M. Butwill, J.P. Zbilut, C.L. Webber Jr., Phys. Lett. A 305 (2002) 59.

[5] N. Marwan, M.C. Romano, M. Thiel, J. Kurths, Phys. Rep. 438 (5–6) (2007) 237.

[6] C. Chatfield, The Analysis of Time Series, sixth ed., Chapman & Hall/CRC, 2003.

[7] N.H. Packard, J.P. Crutchfield, J.D. Farmer, R.S. Shaw, Phys. Rev. Lett. 45 (9) (1980) 712.

[8] G.K. Rohde, J.M. Nichols, B.M. Dissinger, F. Bucholtz, Physica D 237 (5) (2008) 619.

[9] N. Marwan, J. Kurths, Phys. Lett. A 302 (5–6) (2002) 299.

[10] D.P. Lathrop, E.J. Kostelich, Phys. Rev. A 40 (7) (1989) 4028.

[11] Original experimental data retrieved at http://complex.umd.edu/interestingdata/, on 7/7/2008.

[12] M.C. Romano, M. Thiel, J. Kurths, I.Z. Kiss, J. Hudson, Europhys. Lett. 71 (2005) 466.

[13] T.S. Parker, L.O. Chua, Practical Numerical Algorithms for Chaotic Systems, Springer, 1989.